Relief gratings and microlenses fabricated with silicone

Sergio Calixto*

Centro de Investigaciones en Optica A.C., Loma del Bosque 115, Leon, Guanajuato, Codigo Postal 37150, Mexico

*Corresponding author: scalixto@foton.cio.mx

Received 27 November 2006; revised 26 March 2007; accepted 29 March 2007;
posted 30 March 2007 (Doc. ID 77262); published 9 July 2007

Divergent microlenses and low-spatial-frequency interference gratings have been fabricated in low-cost silicone layers. The size of the microlenses ranges from ~1 mm to 100 μm while spatial frequencies of interference gratings range from 4 to 18 l/mm. The fabrication method involves the recording of spatial distributions of mid-IR light. At recording time silicone layers are in a gel state. Then layers are cured by heat. The final silicone layers are transparent and rigid. © 2007 Optical Society of America

OCIS codes: 090.2900, 350.3950.

1. Introduction

Common methods to fabricate microelements involve the use of ultraviolet light [1–6]. Materials that are used with this fabrication method are, for example, photopolymers, photoresist, and dichromated gelatin. On the other end of the spectrum infrared light is also used to make microelements [7–14]. Here we propose the use of mid-IR light ($\lambda = 10.6$ μm) to fabricate microelements. The chosen material is silicone, which after the IR recording is cured on a hot plate.

Siloxanes have good properties that make them a choice over other organic polymers. These properties are good clarity, thermomechanical and photothermal stability, and a number of cure options. Silicones can be formulated to provide dispensable very-low-modulus soft gels and elastomers. They also can be formulated to very rigid resins that can be transfer or injection molded. This range of material options results from the ways in which the basic silicone precursor molecules, consisting of linear, branched, and terminal monomer units, can be combined in a silicone composition [15].

Section 2 describes the silicone mixture preparation method. Section 3 describes the recording of interference patterns that led to the fabrication of interference gratings. A study comprising gratings profiles, their spectra, and diffraction efficiency is also shown in Section 3. Section 4 describes the method to make divergent microlenses. Our results of the tests made to their surfaces and imaging capability are shown.

2. Preparation of IR Sensitive Material

Silicone used in the experiments (Silastic T-2) [16] is a two-component material consisting of a base and a curing agent. A similar material has been used before to replicate relief gratings [17]. The method used to make the silicone layers was the Doctor Blade [18]. In this method a small amount of mixture is placed on a glass plate. Then a blade is passed over the surface leaving a thin film. The film thickness was ~500 μm.

After recording an IR spatial distribution, silicone plates can be cured by leaving them at room temperature for ~6 h or they can be placed over a hot plate with a temperature of 40 °C for ~2 h. Curing is done by an additional reaction. Using higher temperatures could reduce curing time but unfortunately films could suffer a shrinkage, thereby losing fidelity of the recording. At the end of the curing process, silicone films are dry, transparent, rigid, and stable. The operating temperature range is from −45 °C to 200 °C.

3. Recording Interference Patterns

A. Silicone Response to Heat

To study the response of the silicone films to IR interference patterns an interferometric (two-beam)

0003-6935/07/225204-06$15.00/0

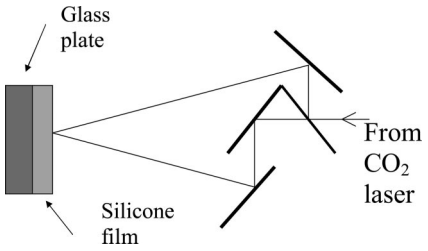

Fig. 1. Optical configuration used to record interference gratings.

study was performed. The light source was a CO_2 laser (Synrad). The IR beam was split with a 50%/50% germanium beam splitter. Three mirrors were used to send the beams to the recording area (Fig. 1). Light parameters in the experiment were the intensity of the two beams at the recording area, beams' intensity ratio, exposure time, and spatial frequency of the interference patterns.

The cross-section intensity of the interfering beams is Gaussian. This means that in the recorded interference pattern, surface modulation is not the same in the whole recording area. Figs. 2(a), 2(b) show the interference pattern captured with a pyroelectric camera. Some Gaussian behavior is shown.

To illustrate the recording process here we present the results when several interference gratings were

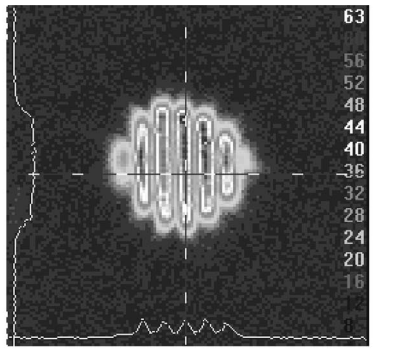

(a)

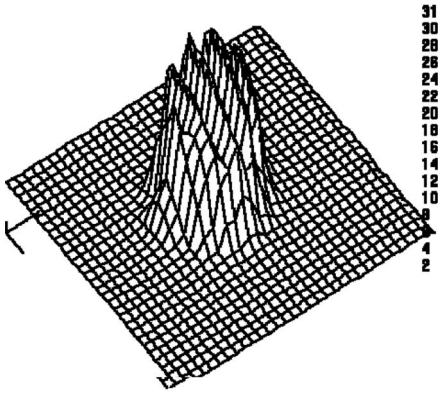

(b)

Fig. 2. (a) Image of the IR interference pattern given by a pyroelectric camera. A three-dimensional plot of the image can be seen in (b).

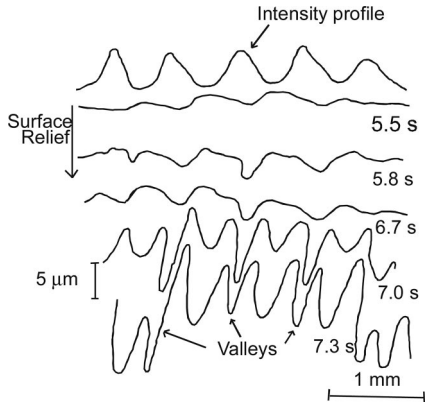

Fig. 3. In the first row the spatial distribution of the IR interference pattern can be seen. Rows 1–5 show surface modulation of five gratings made with different exposure times. Beams' power at recording time was 5 W. Parameter is exposure time.

made. The irradiance of both beams (5 W/cm^2), the beam intensity ratio (1:1), and the spatial frequency of the interference pattern (1.25 l/mm) were kept fixed. The variable was exposure time. After the recordings were made the films were cured. Then the profile of the gratings was studied with a stylus surface analyzer. The results are shown in Fig. 3. The intensity profile of the interference pattern is shown in the upper part of the figure. The absorption of IR light by silicone films heats the mixture, which becomes soft and, in some places, liquid. This liquid will flow to cooler places [19], causing a concavity in the center of the recording and a bump in the periphery due to the displaced material. The depth of the concavity is a function of the local IR beam intensity, the thickness of the layer, and the exposure time. As indicated in Fig. 3 an exposure time of 5.5 s gives a small modulation. Then as exposure time increases, the modulation becomes larger. This behavior is better seen for exposures of 7 and 7.3 s where the material that formed the concavity (valleys) was forced to the periphery. Another valley is then found between the valleys made by the intensity peaks. In this way an interference grating with a doubled spatial frequency is now present.

B. Silicone Response to the Amount of Recording Energy

The energy density received by silicone films at exposure time is given by the time of exposure (s) multiplied by the power density (W/cm^2) of the recording beams. However, the modulation made with short exposure times, t_{exp}, and high-intensity beams is not the same as that made by long t_{exp} and low-intensity beams even if the energy involved is the same. This is due to the phenomenon of heat transference. When short exposure times and high-intensity beams are used most of the energy will remain localized and will not be transferred to the surroundings. To test silicone films with short exposure times, exposures of the order of milliseconds were given. The beams' power density was increased to 10 W/cm^2. The exposure times were

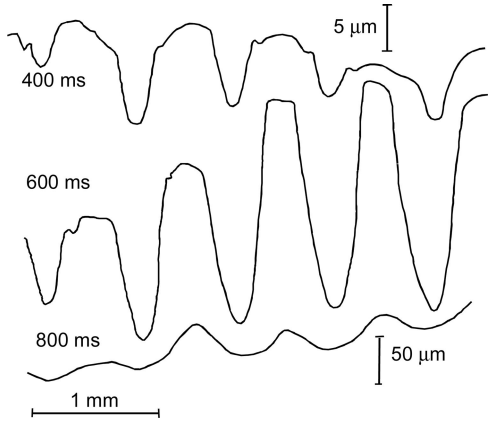

Fig. 4. Surface modulation of three gratings made when the power of interfering beams was 10 W. Parameter is exposure time. Notice that graph at the bottom is in a different scale.

400, 600, and 800 ms. Our results can be seen in Fig. 4. When we compare the maximum depth modulation (~38.8 μm) of the grating made with 800 ms with the maximum depth modulation (~18.7 μm) of the grating made with 7.3 s (Fig. 3) we can see that bigger modulations can be made with short exposure times and high-intensity beams. Concerning energy density we have used about 8 J/cm^2 (800 ms × 10 W/cm^2) to make the grating in Fig. 4 and 36.5 J/cm^2 (7.3 s × 5 W/cm^2) to make the grating in Fig. 3. Aside from this increase in the modulation the phenomenon of doubling the frequency of the grating shown in Fig. 3 is not seen.

C. Spatial Frequency Response

The response of silicone films to interference patterns with different spatial frequencies was tested in the following way. Given a spatial frequency, and a beam power of 8 W, a set of diffraction gratings was recorded on a silicone plate. Each grating was recorded with a different exposure time. Then the recording plate was cured. The diffraction efficiency of the gratings was measured by sending a beam from a He–Ne laser. A series of diffracted orders was seen [Fig. 5(a)]. Intensity in the first order was measured, and the diffraction efficiency of each grating was obtained. A plot describing the behavior of the diffraction efficiency as a function of exposure time for each set of gratings made with a given spatial frequency can be seen in Fig. 5(b). The arbitrary values of the spatial frequencies were 5.6, 7.9, 11.2, 13, and 18 l/mm. Figure 5(b) shows that most of the graphs display the following behavior. For low exposure times diffraction efficiency is low. Then, as exposure time grows, diffraction efficiency also grows to a maximum and then decays. If we take the maximum diffraction efficiency for each spatial frequency and plot it as a function of the spatial frequency we can get the graph shown in Fig. 6. One can see that 18 l/mm is the highest value of the spatial frequency that can be recorded. This limit is because of heat transference in the material that is present between two adjacent heat lines of the interference pattern.

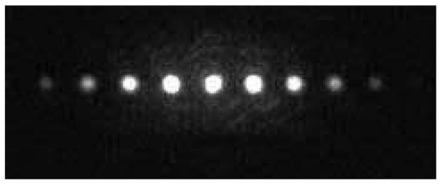

(a)

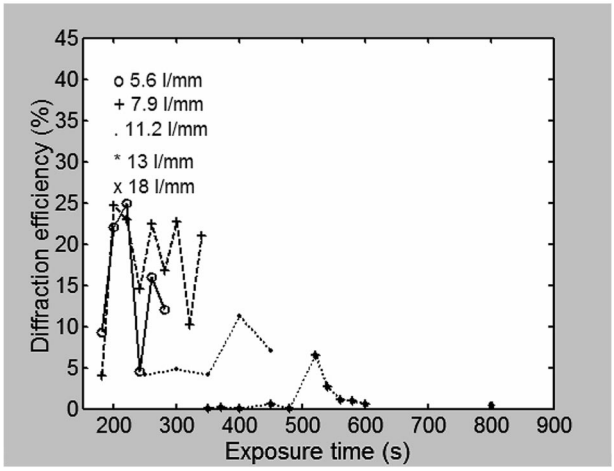

(b)

Fig. 5. (a) Diffracted orders given by a fabricated grating when a He–Ne laser illuminated the grating. (b) Diffraction efficiency as a function of exposure time. Parameter is spatial frequency of the interference pattern.

Gratings surfaces with 16.6 l/mm were investigated with an atomic force microscope. The microscopic image in Fig. 7(a) indicates that the surface shows some roughness. In Fig. 7(b) the profile of the grating is seen with a depth modulation of about 44 nm and a distance from peak to peak of about 60 μm or 16.6 l/mm.

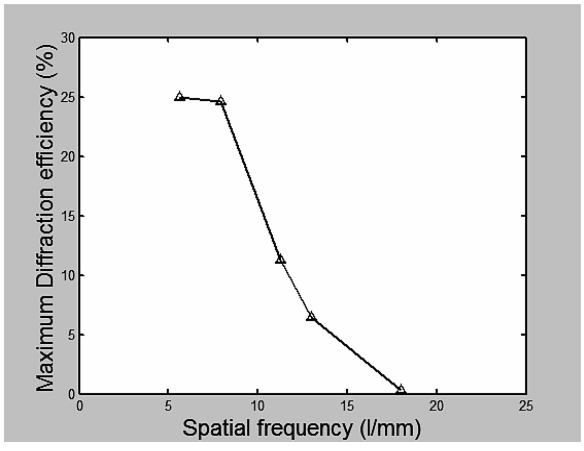

Fig. 6. Maximum diffraction efficiency as a function of spatial frequency.

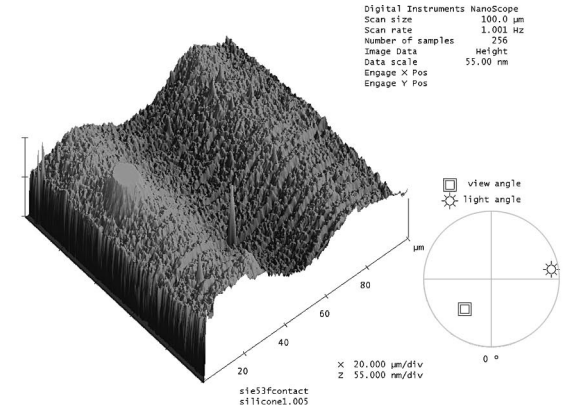

(a)

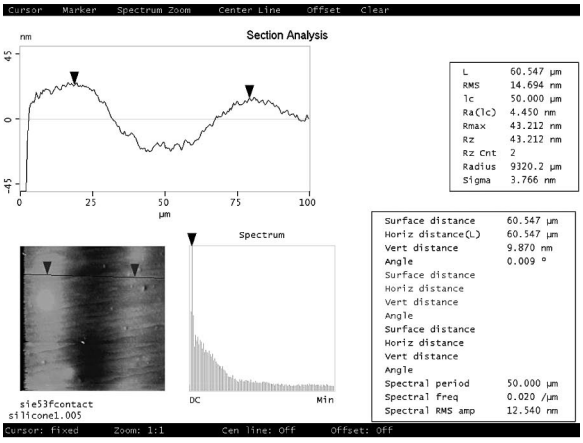

(b)

Fig. 7. (a) Image given by an atomic force microscope of a grating with 16.6 l/mm. (b) Profile of the grating show in (a).

D. Silicone Response to Interference Pattern Visibility

In a common interference pattern the visibility of the fringes can change from one area of the pattern to another. This is because of the spatially varying intensity of the interference beams. To find the response of the silicone films to an interference pattern made with two beams, with different intensity, the following experiment was done. Two coherent beams with a beam ratio of 0.37 (1.48 W/4 W) were made to interfere. Then several diffraction gratings were recorded with different exposure times and their diffraction efficiency was measured. The results can be seen in Fig. 8. This figure also shows the curve plotted for gratings made with a beam ratio of 1. It is now evident that by decreasing the beam ratio the maximum diffraction efficiency has decreased. It is also noted that more energy is needed to write the gratings. Nevertheless the efficiency behavior remains similar.

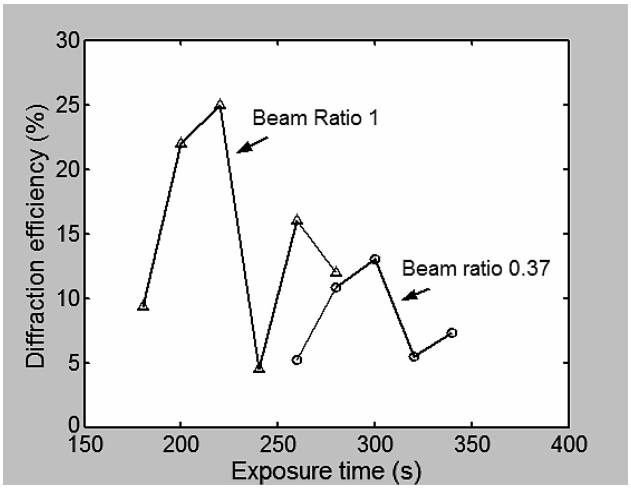

Fig. 8. Diffraction efficiency as a function of exposure time. Parameter is beams' ratio.

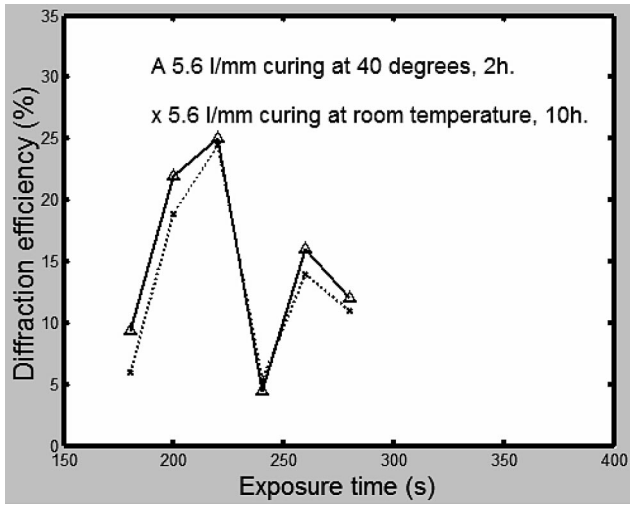

Fig. 9. Diffraction efficiency as a function of exposure time. Parameters are curing time and temperature.

E. Silicone Stability in the Curing Process

Section 2 mentioned that to cure silicone films they were placed on a hot plate at 40 °C for about 2 h. If the curing process is conducted within short times at high temperatures the material could shrink. We performed an experiment to see if the suggested curing process on the hot plate affected the recording. In two different silicone plates a set of gratings was recorded. The spatial frequency and exposure times were the same for both sets. Then one plate was left to cure for about 10 h at room temperature and the other set was cured on a hot plate for 2 h. Diffraction efficiencies of the gratings in each set were measured. Our results are shown in Fig. 9. It is seen that diffraction efficiency curves are similar. This means that recordings made in the plate cured on the hot plate did not suffer deformations.

4. Divergent Microlenses

The silicone mixture was tested to make lenses with diameters from about 1 mm to 100 µm. The following fabrication method was used. The silicon mixture was placed very close to a pinhole. Then light from a CO_2 laser was sent through the pinhole and an exposure was done. The result was the formation of a negative

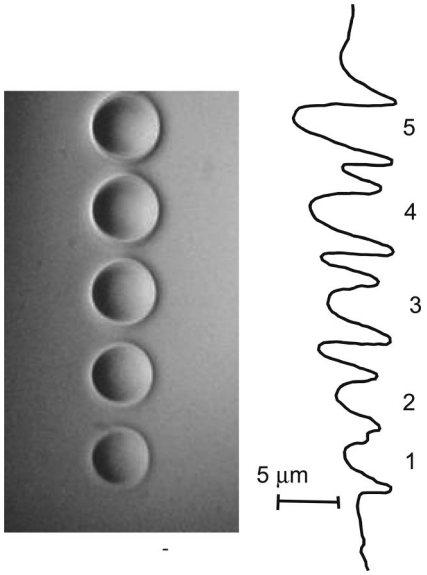

Fig. 10. Set of divergent lenses made with different exposure times and their profiles. Diameter of lenses is ~500 μm.

lens. An example of a set of lenses made with different exposures times and their profiles is shown in Fig. 10.

The back focal distance of microlenses was measured with a microscope. First, the microscope was focused on the surface of the lens. Then it was focused on the image formed by the lens. The distance traveled by the microscope was the back focal distance. Figure 11 shows the behavior of the focal distance as a function of time of exposure for a set of lenses made with a pinhole of 200 μm and a beam power of 10 W.

Microlens arrays can be done by moving the silicone plate with an X-Y-Z micropositioner. Figure 12(a) shows a microarray made with a pinhole with a diameter of 500 μm. Each column was made with a different exposure time. Figure 12(b) shows the images of a triangle given by two columns of microlenses.

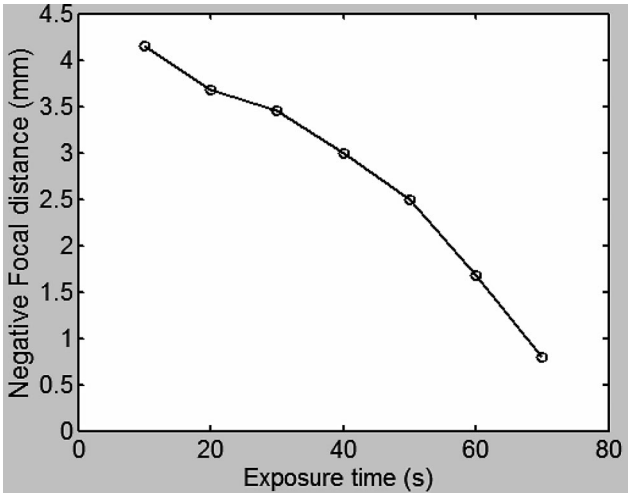

Fig. 11. Behavior of focal distance as a function of exposure time.

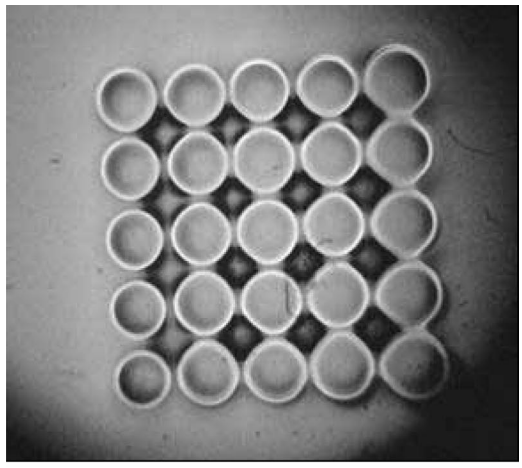

(a)

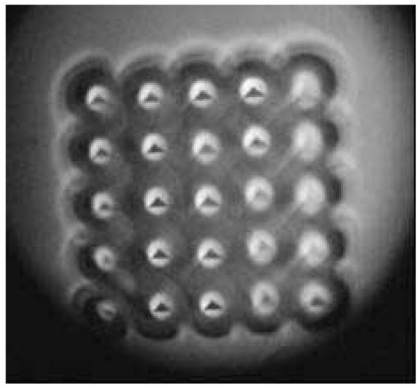

(b)

Fig. 12. (a) Microlens array. Each column shows a set of lenses made with a given exposure time. Diameter of bigger lenses is ~500 μm. (b) Images of a triangle given by some lenses. Lenses in some columns do not show images because they have different focal distances.

5. Conclusions and Comments

We have shown that it is possible to fabricate low-spatial-frequency gratings and divergent lenses in low-cost silicone. The method is based on the recording of spatial distributions of heat on gel-like silicone films. The diffraction efficiency of gratings can reach ~25%. Divergent microlenses with diameters from 1 mm to 100 μm can be fabricated. Lenses with a diameter of 500 μm showed focal distances of about 1–3 mm.

It should be mentioned that silicone material has been used before [11] to make microelements. However, we can find differences with the mentioned work. First, the material that we use now is a monomer with the consistency of a gel at recording time. After recording, films are cured and become rigid. The material used in Ref. 11 was solid from the beginning. Regarding the resolution of the films, gels showed a cutoff frequency of ~18 l/mm. Instead, the cutoff frequency of solid films was ~6 l/mm. Lenses

that can be made with gels are divergent. With solid films the lenses that have been fabricated are positive (plano-convex) and spherical. They were made by melting silicone cylinders.

This work was partially supported by the National Council of Science and Technology (CONACYT, Mexico) under grant 42986-F.

References

1. H. P. Herzig, ed., *Micro-optics, Elements, Systems and Applications* (Taylor and Francis, 1997).
2. C. Croutxe–Barghorn, O. Soppera, and D. J. Lougnot, "Fabrication of microlenses by direct photo-induced crosslinking polymerization," Appl. Surf. Sci. **168,** 89–91 (2000).
3. T. Okamoto, M. Mori, T. Karasawa, S. Hayakawa, I. Seo, and H. Sato, "Ultraviolet-cured polymer microlense array," Appl. Opt. **38,** 2991–2996 (1999).
4. S. Pelissier, D. Blanc, M. P. Andrews, S. I. Najafi, A. V. Tishchenko, and D. Parriaux, "Single-step UV recording of sinusoidal surface gratings in hybrid solgel glasses," Appl. Opt. **38,** 6744–6748 (1999).
5. ⟨http://NANOtechweb.org/articles/news/5/2/10/1⟩, "IBM beats optical lithography limits," 22 February 2006.
6. T. P. Sosnowsky and H. Kogelnik, "Ultraviolet hologram recording in dichromated gelatin," Appl. Opt. **9,** 2186–2187 (1970).
7. C. Roychoudhury and B. J. Thompson, "Infrared holography with 4-Z emulsion," Opt. Commun. **10,** 23–25 (1974).
8. M. Wakaki, Y. Komachi, and G. Kanai, "Microlenses and microlens arrays formed on a glass plate by use of a CO_2 laser," Appl. Opt. **37,** 627–631 (1998).
9. S. Calixto, "Infrared recording with gelatin films," Appl. Opt. **27,** 1977–1983 (1988).
10. J. E. Julia and J. C. Soriano, "On-line monitoring of one-step laser fabrication of micro-optical components," Appl. Opt. **40,** 3220–3224 (2001).
11. S. Calixto, "Silicone microlenses and interferometric gratings," Appl. Opt. **41,** 3355–3361 (2002).
12. S. Kobayashi and K. Kurihara, "Infrared holography with wax and gelatin film," Appl. Phys. Lett. **19,** 482–484 (1971).
13. J. Lewandowski, B. Mongeau, and M. Cormier, "Real-time interferometry using IR holography on oil films," Appl. Opt. **23,** 242–243 (1984).
14. M. Rioux, M. Blanchard, M. Cormier, R. Beaulieu, and D. Belanger, "Plastic recording media for holography at 10.6 μm," Appl. Opt. **16,** 1876–1882 (1977).
15. G. Odian, *Principles of Polymerization* (Wiley-Interscience, 1991).
16. Dow Corning Corporation, South Saginaw Road, Midland, Michigan 48686, USA ⟨http://www.dowcorning.com⟩.
17. A. N. Simonov, O. Akhzar-Mehr, and G. Vdovin, "Light scanner based on a viscoelastic stretchable grating," Opt. Lett. **30,** 949–951 (2005).
18. H. M. Smith, ed., *Holographic Recording Materials* (Springer-Verlag, 1977).
19. G. Da Costa and J. Calatroni, "Transient deformation of liquid surfaces by laser-induced thermocapillarity," Appl. Opt. **18,** 233–235 (1979).